Structural study of quasi-one-dimensional vanadium pyroxene $LiVSi_2O_6$ single crystals

Yuto Ishii,[a] Yoshitaka Matsushita,[b] Migaku Oda[a] and Hiroyuki Yoshida[a,*]

[a]*Department of Physics, Hokkaido University, Sapporo 060-0810, Japan*

[b]*National Institute for Materials Science, 1-1 Namiki, Tsukuba, Ibaraki 305-0044, Japan*

Abstract

Single crystals of quasi-one-dimensional vanadium pyroxene $LiVSi_2O_6$ were synthesized and the crystal structures at 293 K and 113 K were studied using X-ray diffraction experiments. We found a structural phase transition from the room-temperature crystal structure with space group $C2/c$ to a low-temperature structure with space group $P2_1/c$, resulting from a rotational displacement of SiO_4 tetrahedra. The temperature dependence of magnetic susceptibility shows a broad maximum around 116 K, suggesting an opening of the Haldane gap expected for one-dimensional antiferromagnets with $S = 1$. However, an antiferromagnetic long-range order was developed below 24 K, probably caused by a weak inter-chain magnetic coupling in the compound.

Keywords

Pyroxene, Structural phase transition, Single crystal X-ray diffraction, quasi one-dimensional antiferromagnet

Introduction

One-dimensional antiferromagnets have been a fascinating field for searching for novel quantum phenomena. Generally, it is known that the ground state of a one-dimensional (1D) Heisenberg antiferomagnet (AFM) with classical spins is a Néel ordered state. However, in 1D quantum AFMs a Néel state is easily broken by low dimensionality and strong quantum fluctuations, resulting in novel quantum many-body states such as a resonating valence bond (RVB) state.

Theoretically, various ground states of 1D AFMs with uniform nearest-neighbor magnetic interactions dependent on the value of spins are expected to be realized. Spin liquid states with gapless excitations have been realized in 1D AFMs with half-integer spins such as the Bonner-Fischer model [1]. However, in systems with integer spins, the valence bond (spin singlet) state, in which the valence bonds between adjacent spins are arranged periodically, appears as a ground state. Particularly, the systems with $S = 1$ are called Haldane antiferromagnetic chains [2]. The excitation spectrum of the valence bond solid state possesses an energy gap, called a spin gap that separates the singlet ground state from the first excitation

triplet state. The Haldane state is one of the quantum disordered states that may have a hidden order; studies of the unusual Haldane AFM have been intensively carried out for several decades. The $Ni(C_2H_8N_2)_2NO(ClO_4)$[3-5] and other Ni compounds such as $(CH_3)_4NNi(NO_2)_3$[6,7] and Y_2BaNiO_5[8,9] with $S = 1$ have been considered candidate materials for Haldane AFMs.

The pyroxene $AM^{3+}B_2O_6$ (A = alkali metal, B = Si or Ge, and M = trivalent transition metal ion) series compounds are one of the representative 1D AFMs [10]. Figure 1 shows the crystal structure of the pyroxene compound that crystallizes in a monoclinic system with space group $C2/c$. The structure consists of edge-sharing MO_6 octahedra forming a quasi-1D zigzag chain along the c-axis connected by nonmagnetic SiO_4 tetrahedra.

The structural and physical properties of the Ti^{3+}, Cr^{3+} and V^{3+} compounds have been reported. Interestingly, $NaTiSi_2O_6$ exhibits symmetry lowering from the monoclinic system $C2/c$ to the triclinic system P-1 at T_s = 210 K [11-13]. In this structural phase transition, dimerization of the Ti^{3+} magnetic ions is induced by the overlapping adjacent d_{xy} orbitals of Ti^{3+} ions within the edge-shared Ti-O zigzag chain. As a result of the dimerization, a spin singlet ground state is realized. This structural and magnetic cooperative transition is expected to be an orbital-assisted spin-Peierls transition [11,14].

In the V pyroxene compound $LiVSi_2O_6$, two electrons of the V^{3+} ion occupy two of the three t_{2g} orbitals, and thus the V^{3+} ions carry $S = 1$ [15]. According to the room-temperature structure, $LiVSi_2O_6$ is considered as a candidate material for S = 1 quasi-1D AFMs. However, G.J. Redhammer *et al*. reported the occurrence of a structural phase transition at 203 K based on a low-temperature X-ray diffraction technique [16,17]. A relationship between a low temperature crystal structure and magnetic properties has not been clarifying.

In this study, single crystals of $LiVSi_2O_6$ were synthesized and their room-temperature (293 K) and low-temperature (113 K) crystal structures were precisely determined using single crystal X-ray diffraction measurements. We report in detail the structural phase transition of $LiVSi_2O_6$ in which the symmetry is lowered from $C2/c$ to $P2_1/c$ resulting from a rotational displacement of nonmagnetic SiO_4 tetrahedra, and discuss the magnetic properties of $LiVSi_2O_6$ with respect to those of $NaTiSi_2O_6$.

Experimental

Single crystals of $LiVSi_2O_6$ were prepared by solid-state reactions with a flux material. Stoichiometric chemical reagents Li_2O_2, V_2O_3, and SiO_2 weighed about 500 mg with a small amount of Sb_2O_3 flux (approximately 100 mg) were mixed and put into a gold capsule to prevent an uninvited reaction between Li_2O_2 and an inner surface of a quartz tube. Then, the capsule was put into a carbon coated quartz tube sealed under evacuation. Without Sb_2O_3 flux

system, any $LiVSi_2O_6$ single crystal was not grown. The tube was heated to 950 °C at a rate of 2.5 °C/min, kept for 24 h, and cooled down to room temperature at a rate of 2.5 °C/min. The products were washed by distilled water, and needle-shaped and pale-green single crystals were obtained. The typical sizes were 2 mm in length. A chemical analysis using electron probe microanalyzer revealed that no trace of Sb was obtained in the crystals.

For crystal structure analysis, a single crystal with 0.20 × 0.06 × 0.06 mm dimensions and a needle shape was selected. Data collections were carried out using Mo-Kα radiation (λ = 0.71073 Å) on a RIGAKU AFC11 Saturn CCD diffractometer with a VariMax confocal X-ray optics system. The sample temperature was controlled by a flash cooling stream using N_2 gas. Cell refinements and data reductions were carried out by using the d*trek program package in the CrystalClear software suite [18]. The structures were solved using SHELXT [19] and refined by full-matrix least squares on F^2 using SHELXL-2014 [20] in the WinGX program package [21]. The magnetic measurement was carried out on the arbitrary oriented single crystals and polycrystalline samples, using a SQUID magnetometer (Quantum Design, Magnetic Properties Measurement System).

Results and Discussion

The structural analysis revealed that $LiVSi_2O_6$ crystallizes in a monoclinic system with lattice constants a = 9.6299(4) Å, b = 8.5850(3) Å, c = 5.3077(2) Å, and β = 109.7160(10)° at 293 K. Laue class 2/m was confirmed from diffraction intensities, and the systematic reflection conditions were $h + k = 2n$ for hkl and $l = 2n$ for $h0l$. In this study, we assumed space group $C2/c$ for a structure model of $LiVSi_2O_6$. The final R values were $R_{obs}(F)$ = 3.3% and $wR_{all}(F^2)$ = 8.05%. We successfully observed symmetry lowering and determined the low-temperature crystal structure of the compound at 113 K. We confirmed that the Laue class 2/m and the systematic reflection conditions was only $l = 2n$ for $h0l$ at low temperature. $LiVSi_2O_6$ crystallizes in space group $P2_1/c$ with lattice constants a = 9.2814(2) Å, b = 8.5893(2) Å, c = 5.27470(10) Å, and β = 103.0990(10)° at 113 K. The final R values were $R_{obs}(F)$ = 3.38% and $wR_{all}(F^2)$ = 8.85%. The experimental conditions and refined structural parameters are summarized in Tables 1 and 2, respectively, and the low-temperature crystal structure is illustrated in Fig. 2(a). Crystal structures of our solutions are basically same as those of previous reports [16,17]. Further details on the crystal structure investigations are obtained from the Fachinformationszentrum (FIZ), on quoting the depository number CSD-431203 for high-temperature (HT) phase and CSD-431204 for low-temperature (LT) phase. We also have supplied cif files as supplementary informations.

Figure 3 shows the temperature dependence of magnetic susceptibilities for single crystalline and powder sample of $LiVSi_2O_6$. The susceptibilities obey the Curie-Weiss law in the

high-temperature region with an estimated Weiss temperature Θ_W = -368 K, Curie constant C = 0.99 emuK/mol (p_{eff} = 2.81 μ_B) and χ_0 = -0.00076 emu/mol for crystalline sample and Θ_W = -441 K, C = 1.05 emuK/mol (p_{eff} = 2.90 μ_B) and χ_0 = -0.00045 emu/mol for polycrystalline sample. This indicates that the system is the S = 1 quasi-1D AFM. Although the structural phase transition of the compound occurs at T_s = 203 K [22], there are no anomalies in the magnetic susceptibility around the transition temperature; the slope of the inverse susceptibility does not change at all around the transition temperature. The magnetic susceptibility decreases with the lowering of temperature after exhibiting a broad maximum around 116 K. This behavior implies an opening of the spin gap. However, the tiny anomaly observed at 24 K for both samples indicates that the antiferromagnetic long-range order is stabilized as the ground state of the compound, instead of the gapped state, consistent with previous reports [22, 23].

In this structural phase transition, a coordination environment of V^{3+} ion shows only tiny deformation. The difference between the longest and shortest V-O bond lengths in the VO_6 octahedron is 7.44% in the HT phase and becomes 7.42% in the LT phase. The VO_6 octahedron is slightly distorted from the regular octahedron even in the HT phase; thus, the Jahn-Teller distortion caused by the orbital degree of freedom of the t_{2g} orbital is excluded from being an origin of the structural transition. All the V-V distances in the quai-1D V-O zigzag chain are 3.10663 Å in the HT phase and 3.0941 Å in the LT phase. The discrepancy of the lengths, only 0.4%, is caused by thermal contraction. The most prominent change in this structural phase transition is the manner of the connection of SiO_4 tetrahedra. As shown in Fig. 2(b), the O3 oxygen shared by the SiO_4 tetrahedra forms an almost linear chain along the c-axis with angle $\angle$O-O-O = 179.9° in the HT phase. The O3 site in the HT phase splits into O3 and O5 sites in the LT phase that are shared by the SiO_4 tetrahedra below and above the V-O zigzag chain as shown in Fig. 2(a). The O3(O5) oxygen arrangement clearly deviates from the linear chain in the LT phase with $\angle$O3-O3-O3 = 166.5° and $\angle$O5-O5-O5 = 161.2°, forming a zigzag chain along the c-axis as shown in Fig. 2(c). The twisted modes of Si1 (Si1-O1-O2-O5) and Si2 (Si2-O1-O4-O3) tetrahedra are in the antiphase direction. However, angles of Si-Si-Si and V-V-V show only small changes, with $\angle$Si-Si-Si = 119.2° (HT) and 119.11° for Si1 119.15° for Si2 (LT), and $\angle$V-V-V = 117.4° (HT) and 116.9° (LT). The change in the orientation of SiO_4 tetrahedra is defined as the rotational orientation displacement. As the SiO_4 tetrahedra connects the magnetic V-O zigzag chains, it is reasonably to consider that the structural transition is

driven by the rotational displacement. Several bond lengths and angles are summarized in Table 3.

It is important to compare the structural transition of the V compound $LiVSi_2O_6$ with that of the isostructural Ti pyroxene $NaTiSi_2O_6$ [12]. In $NaTiSi_2O_6$, a rotational displacement of SiO_4 tetrahedra never occurs. The characteristic feature of the transition is the dimerization of Ti^{3+}-Ti^{3+} ions that gives rise to an alternating arrangement of short and long Ti^{3+}-Ti^{3+} bonds within the Ti-O zigzag chain [13, 24]. As shown in the Fig. 4, the d_{xy} orbitals of the t_{2g} level of a Ti^{3+} ion occupied by one electron overlap in the *xy*-plane, stabilizing dimerization of adjacent Ti^{3+} ions. However, in $LiVSi_2O_6$ the V^{3+}-V^{3+} ion distance remains unchanged with the structural phase transition; thus no dimerization of V^{3+} ions arises in this compound. Two electrons of the t_{2g} level of a V^{3+} ion occupy the d_{xy} and d_{yz} orbitals because two V-O (two V-O2 in the HT phase, V-O4 and V-O6 in the LT phase) bonds of the VO_6 octahedra in the *xz*-plane are shorter than the other four bonds. The d_{xy} (d_{yz}) orbitals of adjacent V^{3+} ions overlap with each other in the *xy*- (*yz*-) plane, which is responsible for the uniform magnetic direct exchange interaction within the V-O zigzag chain without any dimerization.

The degree of symmetry lowering is a distinct characteristic of structural phase transitions for both compounds. The symmetry of the Ti compound lowers from the monoclinic $C2/c$ in the HT phase to the triclinic $P\bar{1}$ in the LT phase [12]. On the other hand, in the V compound the symmetry lowers from the $C2/c$ in the HT phase to the $P2_1/c$ in the LT phase, maintaining monoclinic symmetry. Both compounds possess the same structure in the HT phase in which Li (Na) and V (Ti) locate at 4e sites with a site symmetry of two-fold rotational axis along the *b*-axis. It is noted that all the nearest-neighbor V-V distances are the same even below the structural phase transition temperature, and the translational (*c*-glide) symmetry within the V-O zigzag chain along the *c*-axis is maintained in the LT phase, resulting in the $P2_1/c$ LT structure. On the other hand, in the Ti compound both long and short Ti-Ti distances are alternately arranged along the *c*-axis because of dimerization of the Ti^{3+} ions. Thus, the *c*-glide of the Ti compound is violated and the crystal symmetry lowers to the triclinic $P\bar{1}$.

In $LiVSi_2O_6$, the d_{xy} and d_{yz} orbitals uniformly overlapped within the zigzag chain, preventing dimerization. Thus, $LiVSi_2O_6$ forms an $S = 1$ quai-1D AFM. The origin of structural phase transition in $LiVSi_2O_6$ is not a Jahn-Teller distortion but a rotational displacement of SiO_4 tetrahedra. Thus, the electronic state of V^{3+} ion is not influenced by that. No significant difference between crystalline and polycrystalline susceptibility data suggests that only a weak magnetic anisotropy affects the magnetic properties of the compound. By fitting the magnetic susceptibility using the 1D chain model with gap Δ [25], we obtained approximate gap value $\Delta \sim 54.4$ K for crystalline sample and $\Delta \sim 51.6$ K for powder sample. The long-range magnetic order at $T_N = 24$ K for both samples is definitely assisted by an inter-chain magnetic coupling

which perturb a one-dimensional nature of the compound. As the electronic state of V^{3+} ion is t_{2g}, a nearest neighbor magnetic interaction is mediated by the direct exchange interaction via the direct overlap of V^{3+} t_{2g} orbital within the V-O zigzag chain. On the other hand, the inter-chain magnetic interaction is a superexchange interaction through the V-O-O-V or V-SiO_4 molecular orbital-V path as seen in $(VO)_2P_2O_7$. Although the t_{2g} orbital of V^{3+} ion does not directs toward the oxygen ions of VO_6 octahedron, a slight overlap of t_{2g} orbit of V^{3+} and 2*p* orbit of O^{2-} gives rise to a non-negligible inter-chain interaction at low temperature. Nothing is influenced on the electronic state of V^{3+} ion by the rotational displacement of SiO_4, however, it affects the inter-chain magnetic superexchange interaction since the rotation of SiO_4 which connects with adjacent V-O zigzag chains changes a degree of orbital overlap through V-O-O-O or V-SiO_4-V and bond angles between them. Thus, the quantum disordered Haldane state is disturbed by the inter-chain coupling at low temperature resulting in the development of antiferromagnetic long-range order at 24 K.

Conclusion

In summary, we synthesized and studied single crystals of pyroxene compound $LiVSi_2O_6$. Single crystal X-ray diffraction measurements revealed that the low-temperature structure crystallized in a monoclinic system with space group $P2_1/c$ and lattice constants a = 9.2814(2) Å, b = 8.5893(2) Å, c = 5.27470(10) Å, and β = 103.0990(10)°. The origin of the structural transition is a rotational displacement of the SiO_4 tetrahedra that connect the V-O zigzag chains. The nearest-neighbor V^{3+} ions are magnetically coupled uniformly through the overlapping of the d_{xy} and d_{yz} t_{2g} orbitals. Thus, $LiVSi_2O_6$ is a quasi-1D AFM even below the structural transition temperature. Unlike the Ti pyroxene, no change of magnetic properties was observed in the structural transition because of the absence of dimerization of V^{3+} ions in the V-O zigzag chain. The development of a magnetic long-range order is attributed to a weak inter-chain coupling that affects the magnetic properties of $LiVSi_2O_6$.

Acknowledgement

We thank A. Matsumoto (Hokkaido Univ.) for the materials characterization. We also thank M. Miyakawa and K. Yamaura (National Institute for Materials Science) for fruitful discussions. This work was supported by the Grants-in-Aid for Scientific Research from the Japan Society for the Promotion of Science (Grant No. 15K17686 and 26410081).

Reference

1 J. C. Bonner, and M. E. Fisher, Phys. Rev.,1964, **135**, A640.

2 F. D. M. Haldane, Phys. Rev. Lett., 1983, **93A**, 464.

3 J. P. Renard, M. Verdaguer, L. P. Regnault, WAC. Erkelens, J. Rossatmignod, and WG. Stirling, Europhys. Lett., 1987, **3**, 945.

4 K. Katsumata, H. Hori, T. Takeuchi, M. Date, A. Yamagishi, and J. P. Renard, Phys. Rev. Lett., 1989, **63**, 86.

5 Y. Ajiro, T. Goto, H. Kikuchi, T. Sakakibara, and T. Inami, Phys. Rev. Lett., 1989, **63**, 1424.

6 V. Gadet, M. Verdaguer, V. Briois, A. Gleizes, J. P. Renard, P. Beatvillain, C. Chappert, T. Goto, K. Ledang, P. Veillet, Phys. Rev. B, 1991, **44**, 705.

7 T. Takeuchi, H. Hori, T. Yoshida, A. Yamagishi, K. Katsumata, J. P. Renard, V. Gadet, M. Verdaguer, and M. Date, J. Phys. Soc. Jpn., 1992, **61**, 3262.

8 J. Darriet, and L. P. Regnault, Solid State Commn., 1993, **86**, 409.

9 A. P. Ramirez, S. W. Cheong, and M. L. Kaplan, Phys. Rev. Lett., 1994, **72**, 3108.

10 H. Ohashi, T. Fujita, and T. Osawa, J. Jpn. Assoc. Mineral. Petrol. Econ. Geol., 1982, **77**, 305.

11 M. Isobe, E. Ninomiya, A. N. Vasiliev, and U. Ueda, J. Phys. Soc. Jpn., 2002, **71**, 1423.

12 G. J. Redhammer, H. Ohashi, and G. Roth, Acta Cryst., 2003, **B59**, 730.

13 M. J. Konstantinović, J. van den Brink, Z. V. Popović, V. V. Moshchalkov, M. Isobe, and U. Ueda, Phys. Rev. B, 2004, **69**,020409(R).

14 T. Shirakawa, Y. Ohta, and T. Mizokawa, Physica B, 2006, **378-380**, 1056.

15 C. Satto, P. Millet, and J. Galy, Acta Cryst., 1997, **C53**, 1727.

16 G. J. Redhammer, and G. Roth, Z. Kristallogr., 2004, **219**, 278-294.

17 G. J. Redhammer, and G. Roth, Z. Kristallogr., 2004, **219**, 585-605.

18 CrystalClear, Rigaku Corporation, Tokyo, Japan, 2005.

19 G.M. Sheldrick, Acta Cryst., 2015, A**71**, 3.

20 G.M. Sheldrick, Acta Cryst., 2015, C**71**, 3.

21 L.J. Farrugia, J. Appl. Crystallogr., 2012, **45**, 849.

22 A. N. Vasiliev, O. L. Ignatchik, M. Isobe, and U. Ueda, Phys. Rev. B, 2004, **70**, 132415.

23 B. Pedrini, S. Wessel, J. L. Gavilano, H. R. Ott, S. M. Kazakov, and J. Karpinski, Eur. Phys. J. B, 2007, **55**, 219.

24 Z. S. Popović, Z.V. Šljivančanin, and F. R. Vukajlović, Phys. Rev. Lett., 2004, **93**, 036401.

25 M. Troyer, H. Tsunetsugu, and D. Würtz, Phys. Rev. B, 1994, **50**, 13515-13527.

Figures

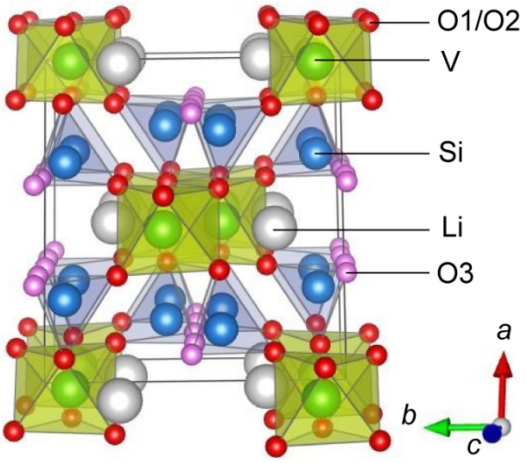

Fig. 1. Crystal structure of $LiVSi_2O_6$ at 293 K determined by single crystal X-ray diffraction experiments.

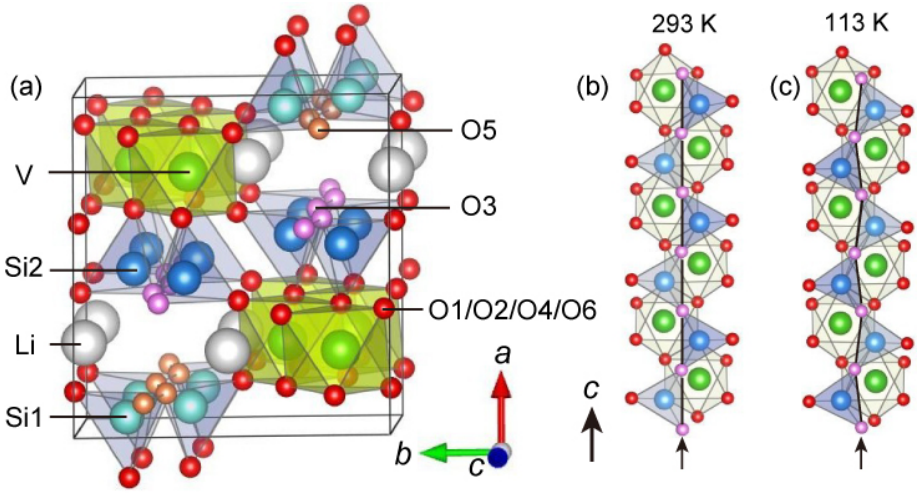

Fig. 2. (a) Low-temperature (113 K) crystal structure of $LiVSi_2O_6$. Schematic illustrations of a quasi-1D zigzag chain consisting of SiO_4 tetrahedra and VO_6 octahedra along the *c*-axis in the HT (b) and LT (c) phases, respectively. The vertical arrows in (b) and (c) indicate the O3 chain of the SiO_4 tetrahedra. The linear O3 arrangement in the HT phase becomes a zigzag chain in the LT phase because of a rotational displacement of the SiO_4 tetrahedra.

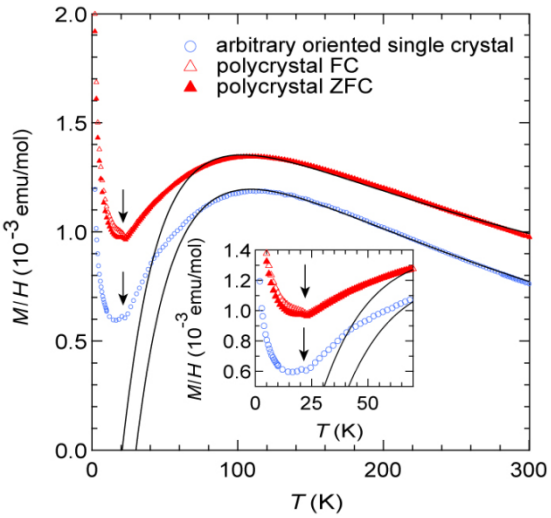

Fig. 3. Temperature dependence of magnetic susceptibility for $LiVSi_2O_6$ in a magnetic field of 0.1 T under a zero-field cooled process. Open circle indicates the data for arbitrary orientated single crystals and solid (ZFC) and open (FC) triangle shows the data for polycrystalline sample. The solid line indicates the fitted result of the 1D magnetic chain model with gap Δ. The inset expands the LT region of the data.

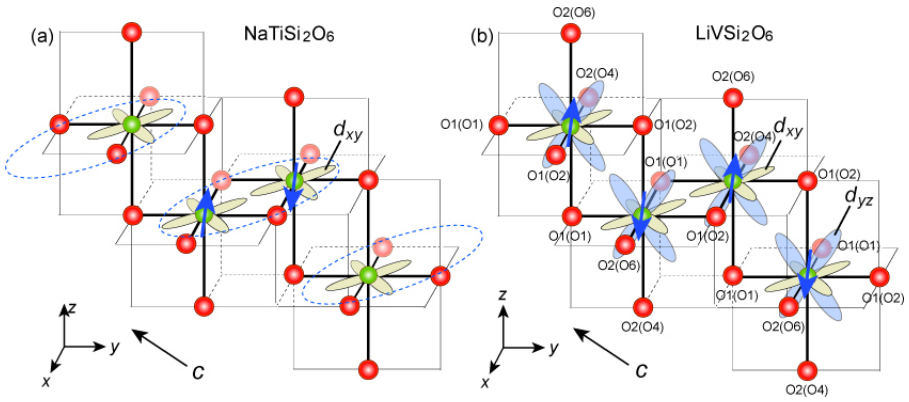

Fig. 4. Schematic pictures of orbital arrangements in the V(Ti)-O quasi-1D zigzag chain along the *c*-axis in $NaTiSi_2O_6$ (a)[11,13] and $LiVSi_2O_6$ (b). The oxygen sites of the V compound in the HT and LT phases (LT phase; in the brackets) are indexed. In the Ti compound, the overlapping of d_{xy} orbitals in the *xy*-plane induces dimerization (dotted ellipses) within the plane, and these dimmers are structurally and magnetically isolated because of the absence of orbital overlapping between dimmers along the *c*-direction. As a result, translational symmetry (*c*-glide) along the *c*-axis is violated. The electron configuration of the V^{3+} ion in $LiVSi_2O_6$ is t_{2g}^2, and the electrons occupy d_{xy} in *xy*-plane and d_{yz} in *yz*-plane. They overlap in the *xy*- and *yz*-plane, and all the V^{3+} ions are connected through this orbital overlapping. Therefore, the system becomes a quai-1D compound along the *c*-axis instead of the dimerization found in the Ti compound.

Tables

Table 1. Crystal data and details of single crystal X-ray diffraction experiments.

Compound	$LiVSi_2O_6$ high temp.	$LiVSi_2O_6$ low temp.
Formula weight (g mol^{-1})	210.06	210.06
Color/shape	pale green/needle	pale green/needle
Crystal dimension(mm)	0.2×0.06×0.06	0.2×0.06×0.06
Temperature (K)	293	113
Space group	$C2/c$	$P2_1/c$
a (Å)	9.6299(4)	9.2814(2)
b (Å)	8.5850(3)	8.5893(2)
c (Å)	5.3077(2)	5.27470(10)
β (deg.)	109.7160(10)	103.0990(10)
Volume ($Å^3$)	413.08(3)	409.561(15)
Z	4	4
D_c (g m^{-3})	3.378	3.407
$F(000)$	408	408
Absorption coefficient (mm^{-1})	2.922	2.947
Radiation	Mo Kα (0.71073 Å)	Mo Kα (0.71073 Å)
Range of h,k,l	h:−13/18, k:-17/17, l:−10/10	h:−13/16, k:-17/17, l:−10/10
Refelctions collected	5433	11025
Independent reflections	1611	3195
Refelctions with $I > 2\sigma(I)$	1562	3009
$R_{obs}(F)$	0.033	0.0338
$wR_{all}(F^2)$	0.0805	0.0885
Goodness of fit	1.289	1.196

Table 2. Final atomic coordinates of the HT and LT $LiVSi_2O_6$.

atom	site	x	y	z	U_{iso} ($Å^2$)	occupation
			293 K			
Li	4e	0.5	-0.2346(4)	-0.75	0.0179(5)	1
V	4e	0.5	0.40594(2)	0.25	0.00419(6)	1
Si	8f	0.70317(3)	0.09067(2)	0.23103(5)	0.00433(6)	1
O1	8f	0.61661(7)	0.58636(6)	0.15523(12)	0.00550(10)	1
O2	8f	0.63092(7)	0.25976(7)	0.17301(12)	0.00904(10)	1
O3	8f	0.64428(8)	0.00286(7)	-0.05807(12)	0.00989(11)	1
			113 K			
Li	4e	1.25059(18)	0.5126(3)	0.9870(3)	0.0100(3)	1
V	4e	0.75024(2)	0.65581(2)	0.51600(3)	0.00276(4)	1
Si1	4e	0.95105(3)	0.34023(2)	0.70676(5)	0.00285(5)	1
Si2	4e	0.54857(3)	0.34017(2)	0.26800(5)	0.00280(5)	1
O1	4e	1.13227(7)	0.33634(6)	0.77351(11)	0.00375(9)	1
O2	4e	0.36786(7)	0.33462(6)	0.19783(11)	0.00386(9)	1
O3	4e	0.60880(7)	0.26817(6)	0.02406(10)	0.00499(9)	1
O4	4e	0.87597(7)	0.50549(6)	0.73136(11)	0.00473(9)	1
O5	4e	0.89477(7)	0.27543(6)	0.41048(11)	0.00526(9)	1
O6	4e	0.61875(7)	0.51013(6)	0.30606(11)	0.00497(9)	1

Table 3. Selected bond lengths (Å) and angles (degree) in the HT and LT phases.

	293 K
V-O1	2.0644(6)×2, 2.0723(6)×2
V-O2	1.9181(7)×2
V-V	3.10663(15)
∠V-V-V	117.3545(0)
∠Si-Si-Si	119.21(4)
∠O3-O3-O3	177.88(7)
	113 K
V-O1	2.0682(6), 2.0689(5)
V-O2	2.0583(5), 2.0669(6)
V-O4	1.9283(6)
V-O6	1.9154(6)
V-V	3.0941(3)
∠V-V-V	116.94(3)
∠Si1-Si1-Si1	119.11(4)
∠Si2-Si2-Si2	119.15(4)
∠O3-O3-O3	166.50(7)
∠O5-O5-O5	161.19(7)